International Journal of Earth Sciences Knowledge and Applications (2022) 4 (3) 380-394

IJESKA contribution to science

International Journal of Earth Sciences Knowledge and Applications
journal homepage: http://www.ijeska.com/index.php/ijeska

Research Article
e-ISSN: 2687-5993

Morphological Studies and Petrogenetic Relationship of Metatexite Cum Diatexite Migmatites Around Buzaye Area, Bauchi, Nigeria

Sadiq Mohammed Salisu[1]*, Ahmed Isah Haruna[1], Maimunatu Halilu[2], Faisal Abdullahi[1] Tahir Garba Ahmad[1]

[1]*Department of Applied Geology, Abubakar Tafawa Balewa University, Bauchi, Nigeria*
[2]*Department of Geology, Moddibo Adama University, Yola Adamawa, Nigeria*

INFORMATION

Article history
Received 19 April 2022
Revised 26 July 2022
Accepted 29 July 2022

Keywords
Migmatites
Buzaye
Diatexite
Schlieren
Stromatic
Pan-African Orogeny

Contact
*Sadiq Mohammed Salisu
sadiqmuhammedsalisu@gmail.com

ABSTRACT

The geology and petrogenetic studies of migmatites around Buzaye area were conducted to evaluate their morphological units and geochemical affinity. Field mapping revealed migmatite with stromatic structures represented the metatexite while parts of the migmatite with schollen and schlieren structures with granitic component represent the diatexite. Fourteen rock samples from different outcrops were cut and examined for geochemical analyses for their major and trace element using XRF pressed pellet technique. Geochemically, diatexite migmatites samples show SiO_2 content from 68.40wt.% to 82.06 wt.% while samples collected from the metatexites has shown silica content as low as 56.42 wt.%. Variation diagrams show negative correlation between MgO, CaO, TiO_2, FeO_2 and Al_2O_3 with SiO_2 but positive correlation with Na_2O and K_2O indicating the normal magma crystallization trends. Based on the major and trace element data, the migmatites in the study area were classified into peraluminous, theolitic and S–type granitoids. On primitive mantle-normalized spider diagrams, all samples show marked negative anomalies in Yb, P and Ti which are similar to that commonly observed in High-K magmas generated along sub-duction zone. Tectonically, the plutons are classified as volcanic arc or subduction related and are late orogenic to post orogenic with respect to the Pan-African Orogeny.

1. Introduction

Granulite facie metamorphic terranes produce different migmatites subdivision due to anatexis processes (Sawyer, 2008). The migmatites are divided into two broad divisions (Brown, 1973): metatexite migmatites and diatexite migmatites.

Metatexites are characterized by the preservation of pre-partial melting structures with centimetre melt segregation in scale. Diatexites are characterized by the disruption of pre-partial melting structures, and are thought to form when the melt content increases to the extent that the solid matrix loses cohesion and the rock gains the rheology of magma. The different morphology between metatexites and diatexites is due to increase in the amount of melt and the estimates of the melt proportion in metatexite and diatexites are commonly in the order of <20% and >20-40 vol.% respective.

The widespread occurrence of migmatites in the Jos-Bauchi transect of higher grade parts of the metamorphic terrane has been noted previously (Dada and Respaut, 1989; Dada et al., 1989; Ferre et al., 1998; Ferre et al., 2002; Ferre and Caby, 2006).

The study area is part of the granulite facies terrain of the Northern Basement Complex, which lies along the Jos - Bauchi transect which is a representative section of the Neoproterozoic Belt of Northern Nigeria (Ferre and Caby, 2006).

The area hosts a lots of migmatites; whose compositional transformation and evolution is poorly known. The area is situated between latitudes N 10º 16’ 00” and N10º 13’ 00” and longitudes 9º 41’ 30” E and 9º 38’ 00” E within sheet 149 Bauchi NE map of the Geological Survey of Nigeria.

The study area covers an approximate area of 35.2 km^2 and is accessible by a major road linking Bauchi to Plateau and numerous footpath to access the remote areas within the study area.

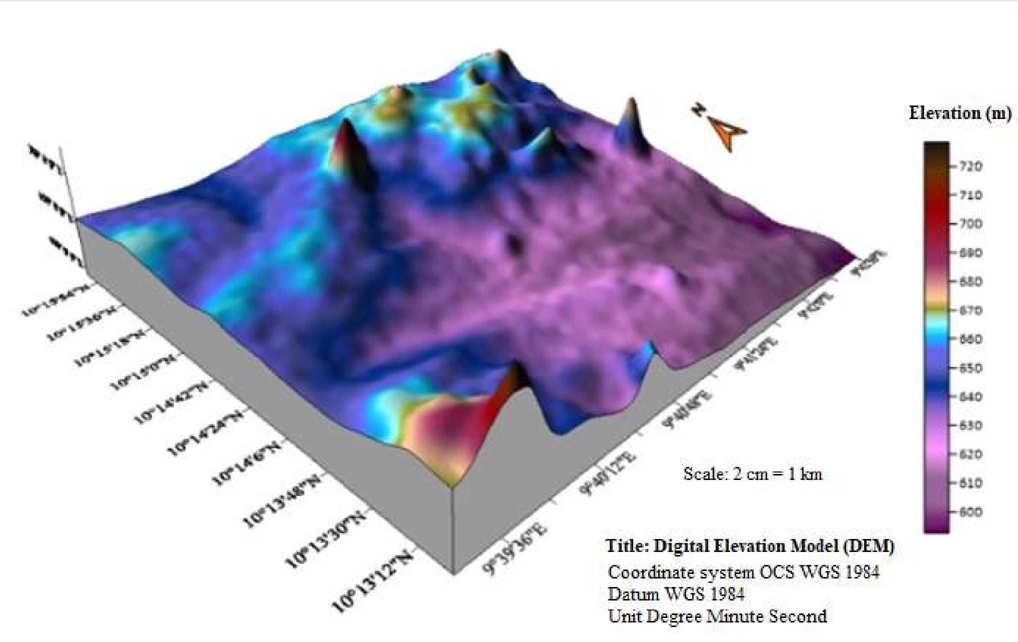

Fig. 1. 3D DEM map of study area

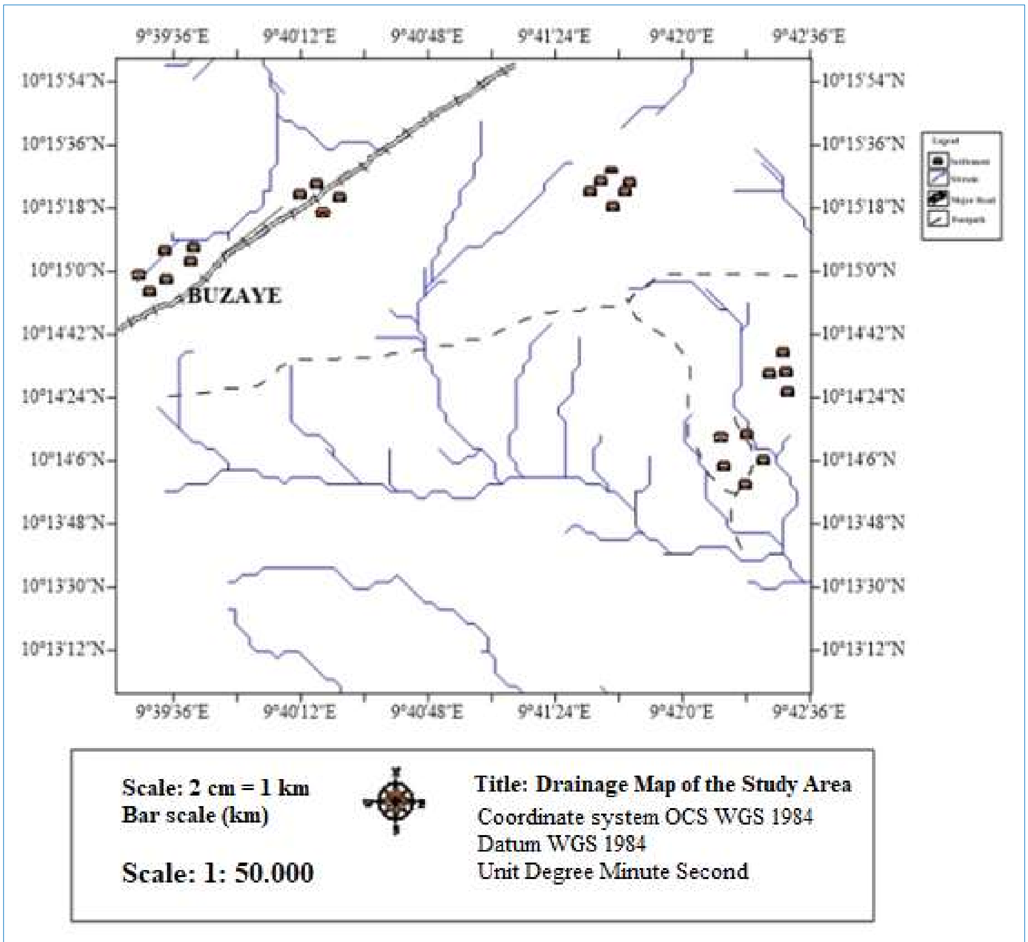

Fig. 2. Drainage map of the study area

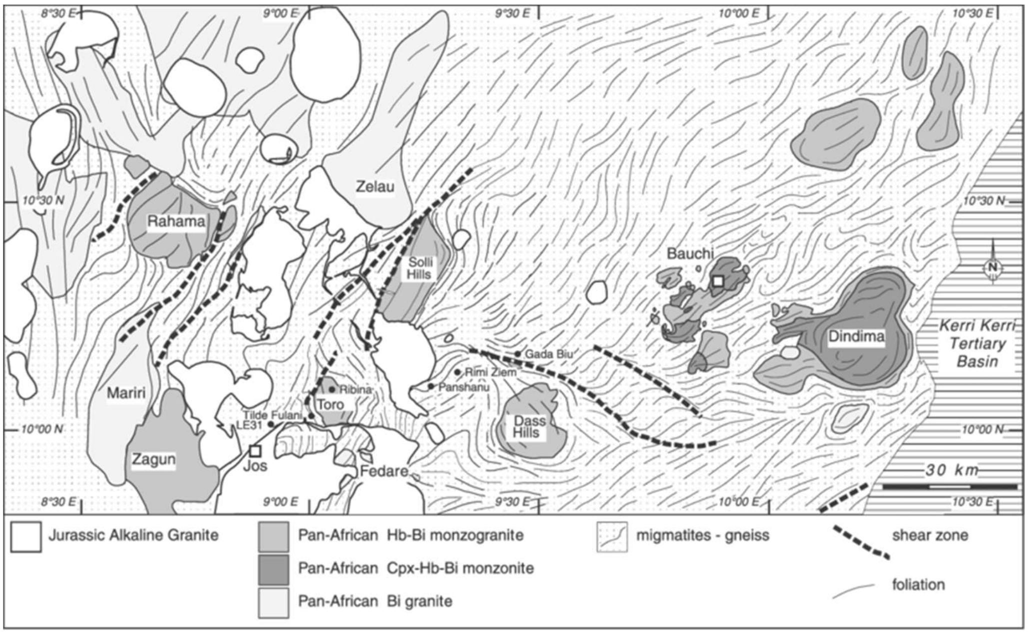

Fig. 3. Geological map of the Jos–Bauchi area. Foliations compiled from field data, SLAR images and previous maps (Wright, 1971)

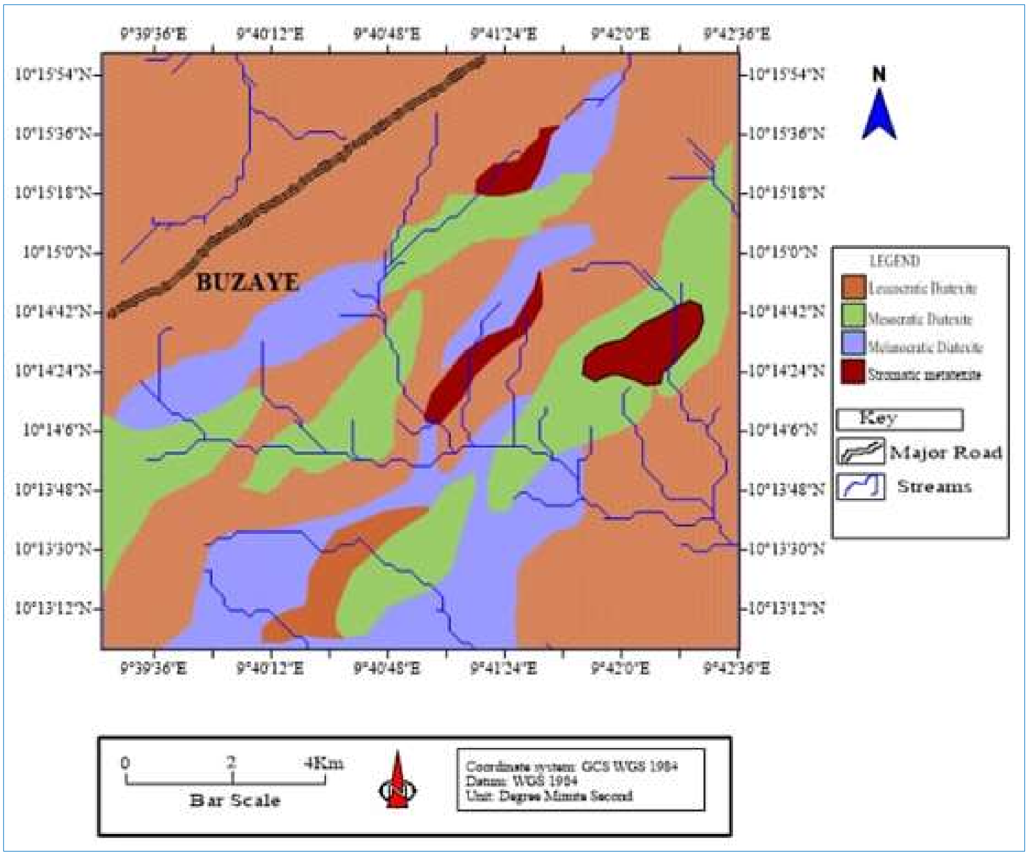

Fig. 4. The geological map of the Buzaye showing the two major rocks types encountered in the area

The study area is characterized by a hilly topography with elevations ranging from 600 to 720 meters above sea level (Fig. 1) and has a dendritic drainage pattern with streams flowing rapidly from one main watershed (Fig. 2). Extensive sampling of metasedimentary gneisses of the area (Jos-Bauchi transect) has revealed several occurrences of granulite facies rocks within high temperature amphibolites facies rocks and anatexites (Ferre and Caby, 2006). Therefore, in this paper, we present different morphological unit of migmatites and a whole rock geochemical affinities of the different migmatite subdivision.

3. Geological Settings

The Neoproterozoic Trans-Saharan Belt in which the study area falls within was suggested to be formed between 700 Ma and 580 Ma by accretion of terranes between the converging West African Craton, the Congo Craton and East Saharan Block, which was probably a craton until 700 Ma (Black and Liegeois, 1993) when it was widely and largely reactivated, except in few areas. The Aïr-Hoggar segment of this belt formed by oblique docking of north-south elongated terranes (Liégeois et al., 1994). The initial lithospheric plate convergence was accommodated along several Neoproterozoic subduction zones (Caby, 2003). The main Pan-African suture is marked in Mali by 620 Ma old high-pressure and locally ultra-high-pressure metamorphic assemblages with preserved coesite (Caby, 1994; Jahn et al., 2001), in Togo by kyanite eclogites and in Ghana by high pressure granulites (Attoh, 1998). The movement of nappes during the initial stage of convergence and crustal thickening was to the west or southwest (Caby, 1989; Castaing et al., 1993). The late-orogenic tectonics are characterized by north-south to NNE dextral strike-slip deformation (Djouadi et al., 1997) mostly localized along continental-scale shear zones and faults, such as the Kandi-$4^0 50'$ fault (Caby, 1989).

The transpressive tectonics and terrane accretion model proposed by Black et al. (1994) for Hoggar, may also apply to Nigeria. The Jos–Bauchi transect situated to the east of the main terrane boundary (Fig. 3), includes mostly gneisses and anatexites of metasedimentary origin (Ferre et al., 1998, 2002).

The depositional age of the sediments is poorly constrained. No basement–cover relationships have been identified. U–Pb zircon ages on syn-kinematic to late kinematic plutons from the Jos–Bauchi area suggest that the Pan-African tectonothermal events took place between 638±3 Ma and 585±7 Ma (Dada and Respaut, 1989; Dada et al., 1989; Ferré et al., 1998; Ferré et al., 2002). Another U–Pb monazite age from the studied area yields an age of 618+10 Ma (Dada et al., 1993). The close relationships between the regional tectono-metamorphic evolution of gneisses, regional anatexis and emplacement of syn-kinematic plutons from the monzodiorite–charnockite association strongly suggest that this area underwent a monocyclic metamorphic history (Ferré et al., 1998). This is in agreement with model ages of 1.8 Ga obtained on Tilde Fulani migmatitic metasedimentary rocks by Dada (1998). It further establishes that the source of the sedimentary rocks is younger than Late Palaeoproterozoic, and strengthens the case for a single monocyclic Pan-African evolution.

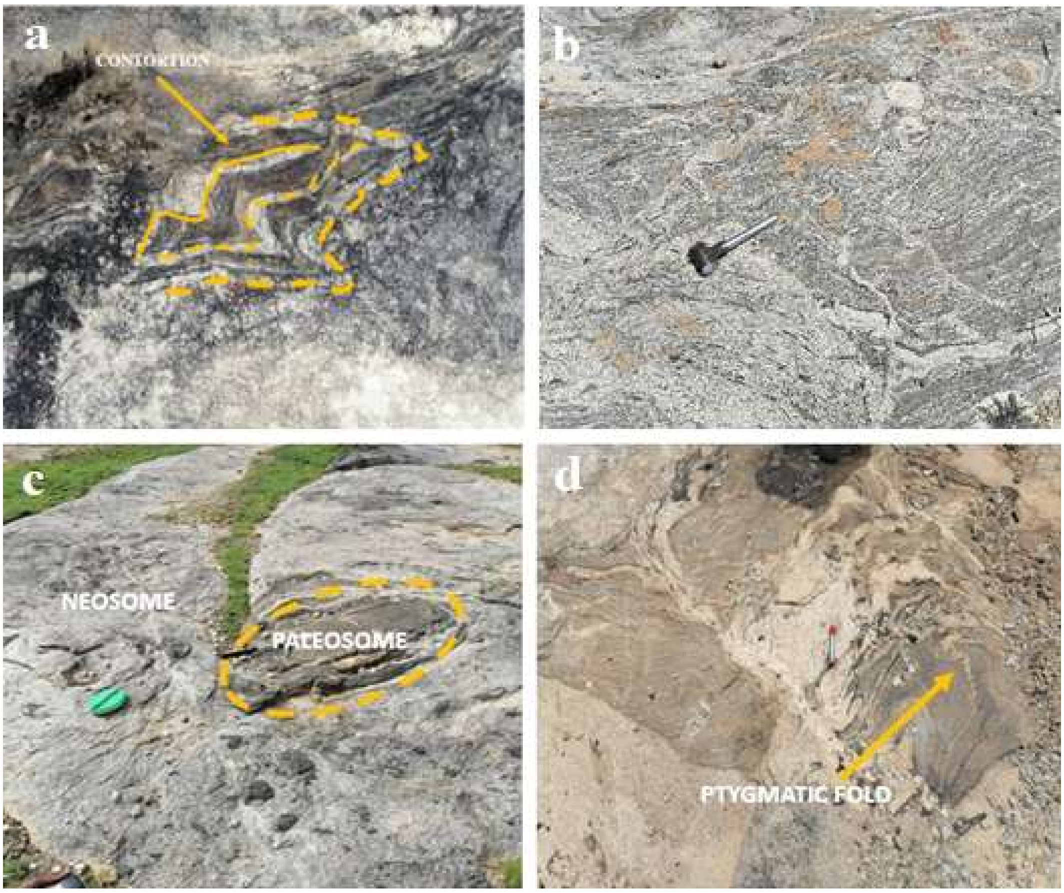

Fig. 5. (a)-(d) Field view of stromatic metatexite forming continuous coarse- to medium-grained layers within the study area, (a)-(b) stromatic metatexite characterized by more or less regular leucosomes sub-parallel to the paleosome, (c) Patch metatexite and (d) Ptygmatic fold

3.Methodology

Detail field observation of the migmatite geology at the scale of the outcrop was conducted. Representative surface rock samples were taken from each migmatites suite according to their mineralogical and lithological variations. A total of thirty surface rock samples were collected from twenty-two suites and data was recorded based on the mineralogical compositions, texture and colour of the rocks with and without the aid of high magnification lens. Geological map for each rock with respective host rocks was performed.

Among these representative surface rock samples fourteen samples were selected for whole rock geochemistry. Fourteen selected samples were resized or reduced by cutting machine to a size of (10×5) cm^2 and were sliced into two parts using rock cutter at thin section laboratory of Applied Geology Department, Abubakar Tafawa Balewa University (one piece for rock geochemistry, and the remaining for reference and stored in laboratory). Several petro-chemical variation diagrams have been employed to discern any relationships or trends which may have bearing on petrogenesis of the various units.

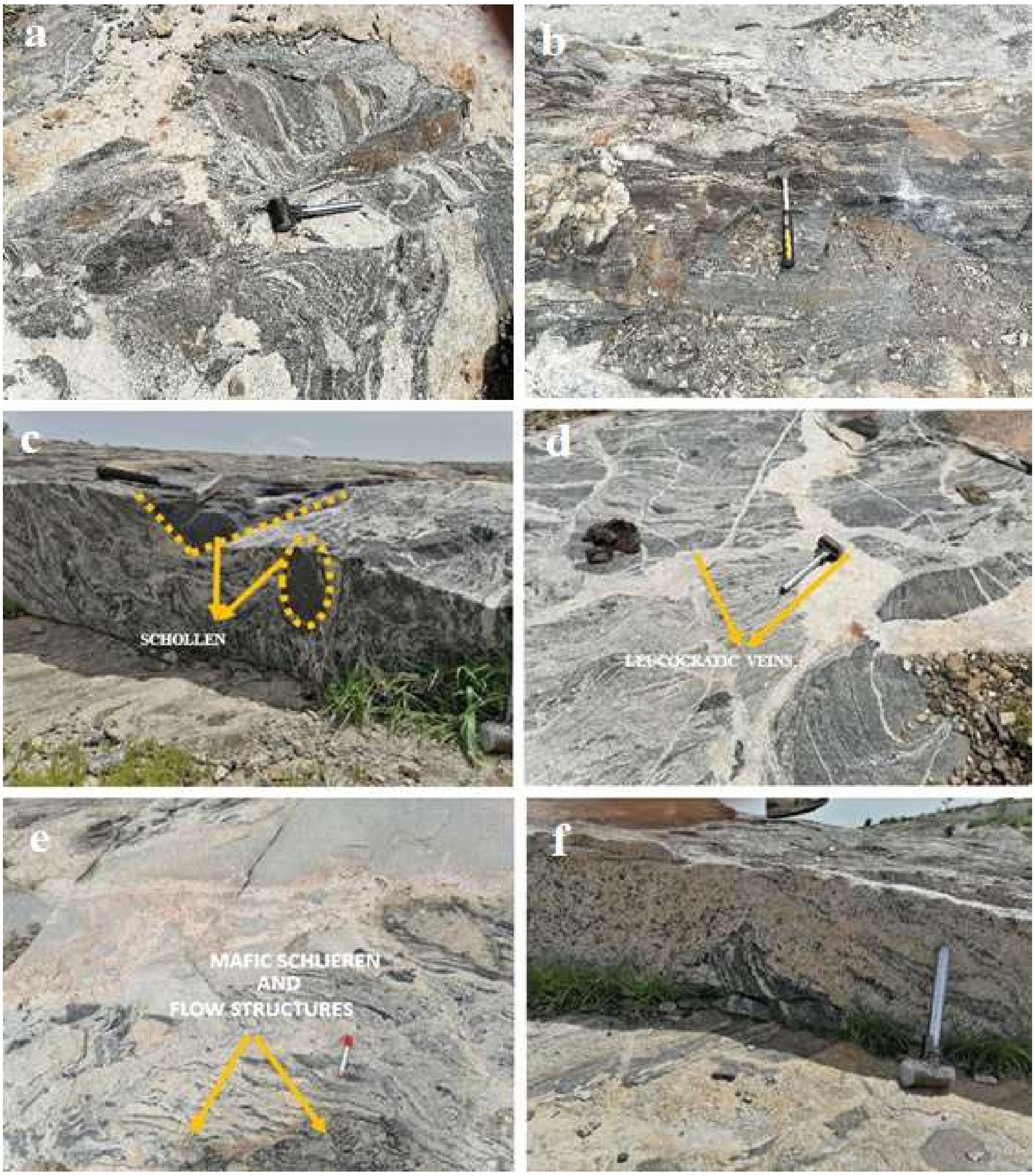

Fig. 6. Field occurrence of diatexite magma: (a)-(b) Melanocratic diatexites, (c) Mesocratic diatexites characterised by the presence of raft-like blocks within mesocratic neosome, (d) Mesocratic diatexites injected with leucocratic veins, (e) Leucocratic diatexite containing magma flow structures with melt segregation and mafic schlieren and (f) Leucocratic diatexite

4. Results and Discussions

4.1. Field relationship and morphology of the migmatites

Field mapping revealed two major migmatite bodies concentrated in the study area which have variable shapes, morphology and structural relationship (Fig. 4).

The migmatites varies from metatexite rocks in which relict primary structures are preserved, to rocks structurally disrupted by the migmatization process known as diatexites. The two types of rocks mapped in the study area includes:

1. Metatexite
2. Diatexite
    a. Mesocratic Diatexite
    b. Melanocratic Diatexite
    c. Leucocratic Diatexite

4.1.1. Metatexite migmatites

The metatexite migmatites exposed in the study area fall within stromatic metatexite of Sawyer (2008) classification. They are characterized with fold structures in which each layer is texturally and mineralogical distinct (Figs. 5a-c), and are found adjacent to diatexite in some outcrops.

They consist of a dark grey, fine-grained (0.2-1 mm), compositionally layered host, which contains a small volume (<30%) of leucocratic portions of quartzofeldspathic composition. Typically, the biotite-rich portion are located at the edges of the leucosomes, and hence represent melanosomes, or mafic salvages. The leucosomes are texturally more homogeneous, and coarser grained than either the melanasome or paleosome, and contain quartz, k-feldspar, plagioclase, and minor biotite.

The majority of leucosomes are parallel to the pre-migmatization structures (foliation and/or primary compositional layering) in their host, but some are cross cutting. The metasedimentary rocks are considered to be the protolith, or paleosome, to the metatexites, as the same type of compositional layering (bedding) and rock types can be recognized on them. The pre-partial melting structures are preserved only in the enclaves, which are locally abundant (Fig. 5c).

Table 1. Geochemical result for analyzed migmatites

	Metatexite		Melanocratic Diatexite			Mesocratic Diatexite					Leucocratic Diatexite		
	C 1	**A 1**	**F 2**	**G 2**	**E 2**	**D 3**	**A 3**	**D 2**	**D 1**	**E1**	**A 2**	**B 1**	**B 2**	**G 1**
Oxides (%)														
SiO_2	56.42	60.11	68.4	72.02	72.08	73.08	74.4	74.64	75.5	76.66	72.34	78.5	80.6	82.06
CaO	0.43	0.12	0.22	0.12	0.1	0.2	0.43	0.24	0.08	0.03	0.1	0.06	0.01	0.08
MgO	0.06	0.64	0.03	0.02	0.01	2.01	0.08	0.03	0.02	ND	ND	ND	ND	ND
SO_3	0.12	0.03	ND	0.004	ND	0.03	ND	ND	ND	ND	ND	ND	ND	ND
K_2O	0.48	0.8	0.34	0.92	1.1	0.8	1.26	2.6	0.82	0.52	8.41	3.04	3.24	0.84
Na_2O	2.03	2.46	2	2	2.01	1.64	2	1.52	1.67	1.94	0.34	1.64	0.62	0.42
TiO_2	1.34	1.21	1	0.87	0.79	0.24	1.2	0.48	0.73	0.09	0.43	0.73	0.21	0.12
MnO	0.12	0.3	0.06	0.03	0.04	0.06	0.04	ND	0.08	0.04	0.03	0.06	ND	ND
P_2O_5	0.06	0.05	0.02	ND	ND	0.01	ND	ND	ND	ND	ND	ND	ND	ND
Fe_2O_3	21.2	18.01	14.01	10.06	9.86	5.48	4.84	4.43	5.45	14.01	2.01	2.04	1.64	3.34
$A_{l2}O_3$	14.84	12.43	12.42	12.4	12.7	13.76	13.66	12.82	13.55	13	14.06	12.4	12.64	12
H_2O	0	0	2.2	1.42	1.4	0	0	0	0	0	0	0	0	1.01
Elements (ppm)														
V	398.06	720	709	720	420	254	399	502	400	518	520	501.01	283	660
Cr	710.1	212.02	342.87	432.06	610.4	648.29	220	425	530.1	945	677	318.02	614.2	616
Cu	460	425	180	240	280	330	350	290	340	330	360	480	379	380
Sr	1020	2230	110	1790	1000	1220	2050	290	1450	2030	493	1890	980	1830
Zr	7340	1600	730	2000	1000	1200	4310	720	1000	1500	2700	5720	940	1200
Ba	1030	690	900.88	1000	600	3100	200	100	900	1800	8400	680	700	2010
Zn	1300	58	20	460	160	97	380	50	30	560	190	100	60	370
Ce	77	58.03	54	20	80	50	50	45	42	54	39.88	30	44	63
Pb	47	84	70..88	23.99	580	26	92	17	25	867	31	75	9.09	56.09
Bi	2.033	0.451	0.66	10	3.98	0.099	1.023	0.219	0.89	0.873	0.045	0.344	1.012	5
Ga	31	26	12	4	6	39	24	17.4	22	22	9	34.02	19.9	5.09
As	4	15.05	21	4.08	0.46	7.02	9	7	15	17	6	22	11	3
Y	87	2.9	24	19	26	15	28	39	15	3.9	20	10	28	4.3
Ir	5.6	2.06	28	4.6	3.8	20	4.5	3.1	3.1	6.09	1	5.1	30	2.02
Au	0.039	0.43	0.8	1.9	1.6	0.22	0.2	0.014	0.224	0.488	0.37	0.67	0.021	0.2
Ni	0.011	<0.001	<0.001	<0.001	<0.001	<0.001	<0.001	<0.001	0.038	<0.001	<0.001	0.056	<0.001	<0.001
Rb	13	39	27	47	62	29	17	9.84	30	30	86	21.6	5.5	36
Mo	0.008	<0.001	<0.001	0.01	0.008	<0.001	0.21	0.01	0.009	0.2	0.345	<0.001	<0.001	0.009
Co	1.003	5	1.003	0.034	0.998	0.034	0.877	<0.001	0.998	1.094	<0.001	0.09	0.345	<0.001
Cd	<0.001	<0.001	0.002	<0.001	<0.001	0.005	<0.001	<0.001	0.002	<0.001	8.7	0.032	0.008	0.005
Ru	4.42	8.6	5.07	0.98	0.98	0.12	0.87	0.82	1.26	2.06	30	0.65	1.03	1.23
Eu	23	38	57	33	23	180	33	120	120	36	0.004	160	16	340
Re	0.008	<0.001	0.006	<0.001	0.004	<0.001	<0.011	<0.001	0.002	0.045	24.09	<0.001	0.006	<0.001
Nb	11	18.001	10	20	60	32.01	76	14	48	83	20.1	15	40.03	42
Ag	1.4	1.2	0.87	0.48	1.12	0.41	0.032	0.67	1.12	0.09	1.3	0.6	0.55	0.54
Ta	40.24	41.2	38	15	101	42,10	81	64	36	64	64.09	70.2	61	55
W	12.3	0.882	7.84	2.45	5.62	0.891	4.34	13.3	0.96	1.46	3.99	12	6.066	5.06
Hf	18.09	11	6.62	9.09	28	33	51	16	20	21	14	39.45	20.4	24
Yb	0.46	5.9	2.04	2.31	0.19	4.04	0.98	1.76	2.11	6.9	0.96	2.14	0.09	0.46
In	4.1	8	3.5	1.8	2.8	2.1	1.5	3	1.9	0.09	5.2	9.72	2.3	2.23
Se	0.1	<0.001	0.1	<0.001	0.22	<0.001	0.034	0.28	0.21	0.012	0.25	0.2	0.2	0.28
U	<0.001	<0.001	0.101	0.042	0.025	<0.001	0.01	<0.001	0.022	0.007	0.21	0.201	0.005	<0.001
Th	1.03	0.2	0.24	0.18	0.09	2.5	0.1	0.56	0.86	2.2	0.22	0.21	0.28	0.31
Sb	10	3.24	0,55	1.08	2.24	7.03	7	12	6.13	14	0.3	8.01	4.04	3.3
Ge	4.06	68	14.41	4.4	8.8	200	90	4	4	40	90.6	14.01	8	4.36
Sn	40.55	43.4	42.55	21.06	27.03	31.06	39.12	9.88	17.03	20.12	47.23	61.22	48.23	19.88

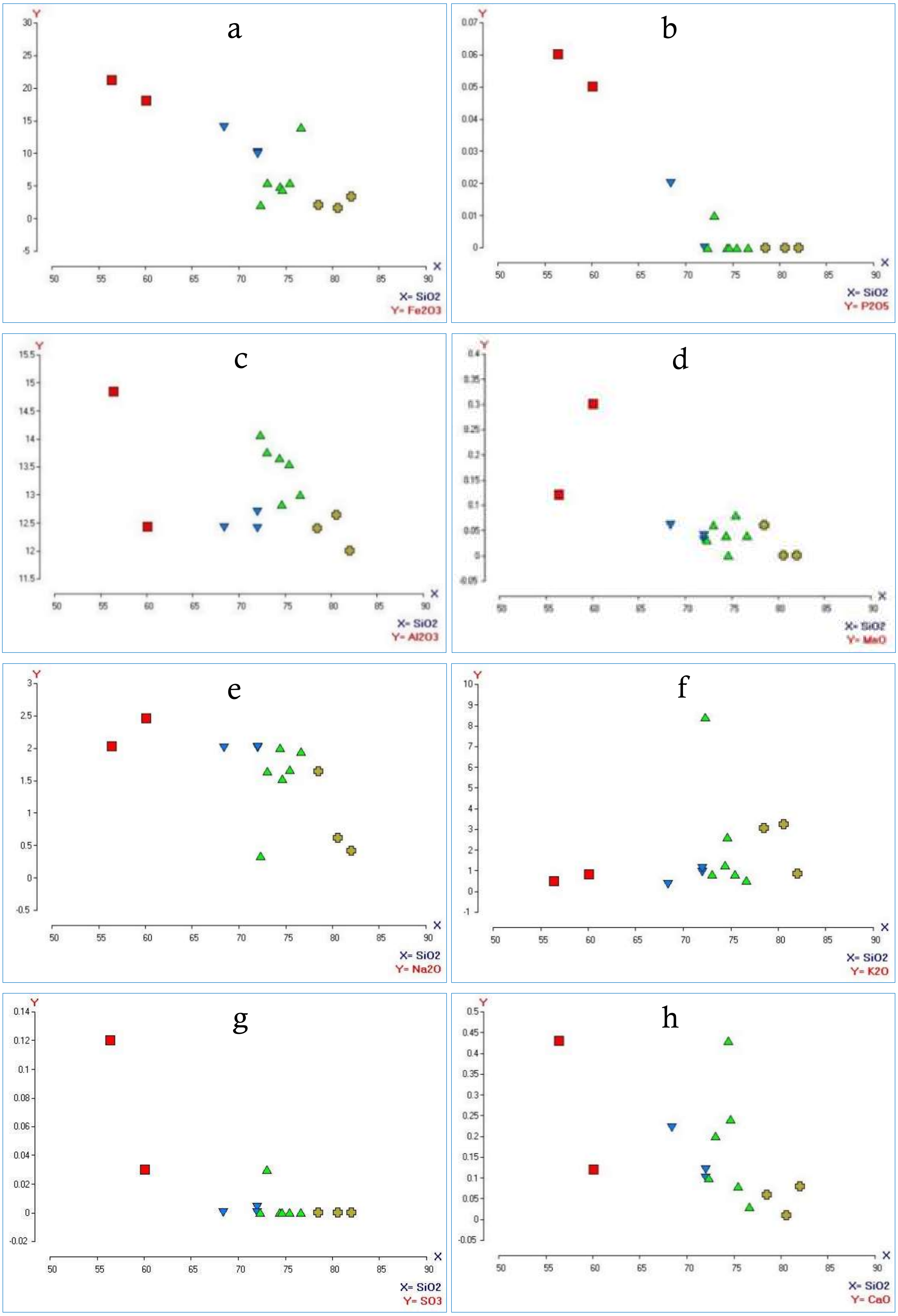
a
X= SiO2
Y= Fe2O3
b
X= SiO2
Y= P2O5
c
X= SiO2
Y= Al2O3
d
X= SiO2
Y= MnO
e
X= SiO2
Y= Na2O
f
X= SiO2
Y= K2O
g
X= SiO2
Y= SO3
h
X= SiO2
Y= CaO

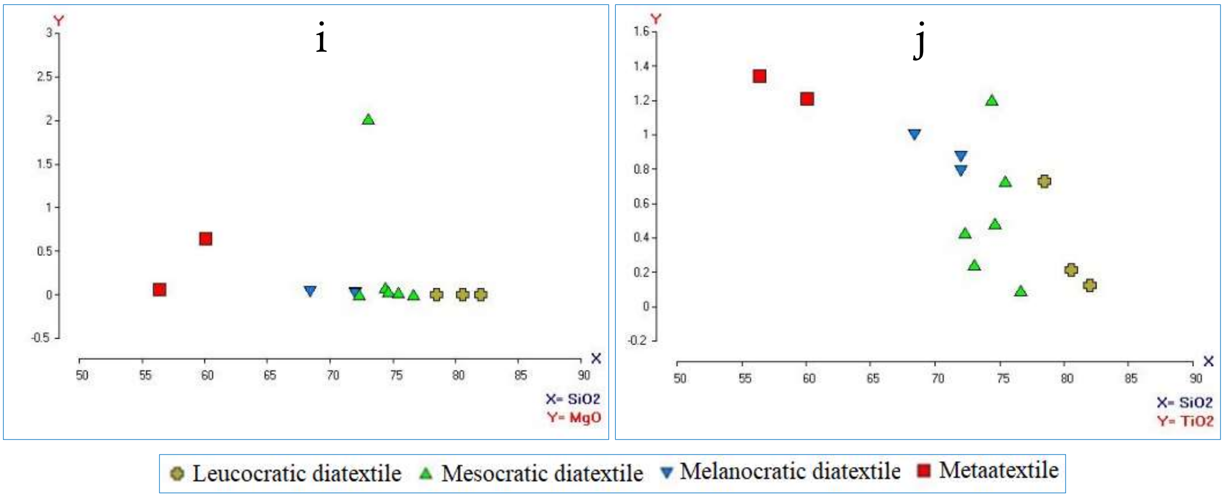

Fig. 7. Harker variation diagram of silica (SiO_2) versus major oxides for samples from different migmatite sites

4.1.2. Diatexite migmatites

Diatexites is the most abundant migmatite type in the study area and form layers up to tens of metre thick and occur as sheet-like bodies, they show a considerable range in morphology from mesocratic to melanocratic through to leucocratic diatexites (Figs. 6a-f). In general, diatexite migmatite in the study area is characterized by increased grain size (0.5-5mm), relative to either metasedimentary paleosome or the metatexite and show no clear banding or gneissosity. Pre-migmatization structures are absent from the neosome, and commonly replaced by syn-anatectic flow structures (Fig. 6). The palaesome can occur as rafts or schollen, or it may be absent (Fig. 6c).

However, it is clear that the field relations of diatexites in the study often indicate bulk flow with produced dark-light-coloured schlieren enriched in biotite and plagioclase respectively (Fig. 6e).

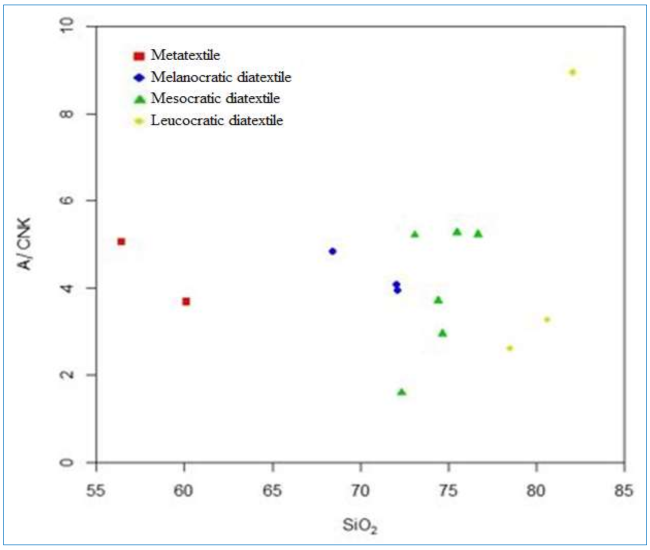

Fig. 8. SiO_2 versus $Al_2O_3/(CaO + Na_2O + K_2O)$ diagram for samples from different migmatite sites

All have undergone a textural homogenization that has destroyed the primary centimeter bedding typical of the metasedimentary rock and the metatexite and have plutonic igneous textures. The loss of pre-migmatization structures and further development of flow structures suggests that a larger melt fraction was present in these rocks compared with the metatexites.

Some diatexite masses are injected with leucocratic veins or dikes from a few centimeters to 30cm wide (Fig. 6d). There are systematic mineralogical and textural variation within diatexite migmatites, and three subdivisions are made.

4.2. Geochemistry

A total of fourteen (14) representative samples were analysed for whole rock geochemical analyses using X-Ray Fluorescence (XRF). Major and trace element contents have been determined on 2 metatexites, 3 melanocratic diatexites, 6 mesocratic diatexites, and 3 leucocratic diatexites. The results of the analyses are represented in Table 1.

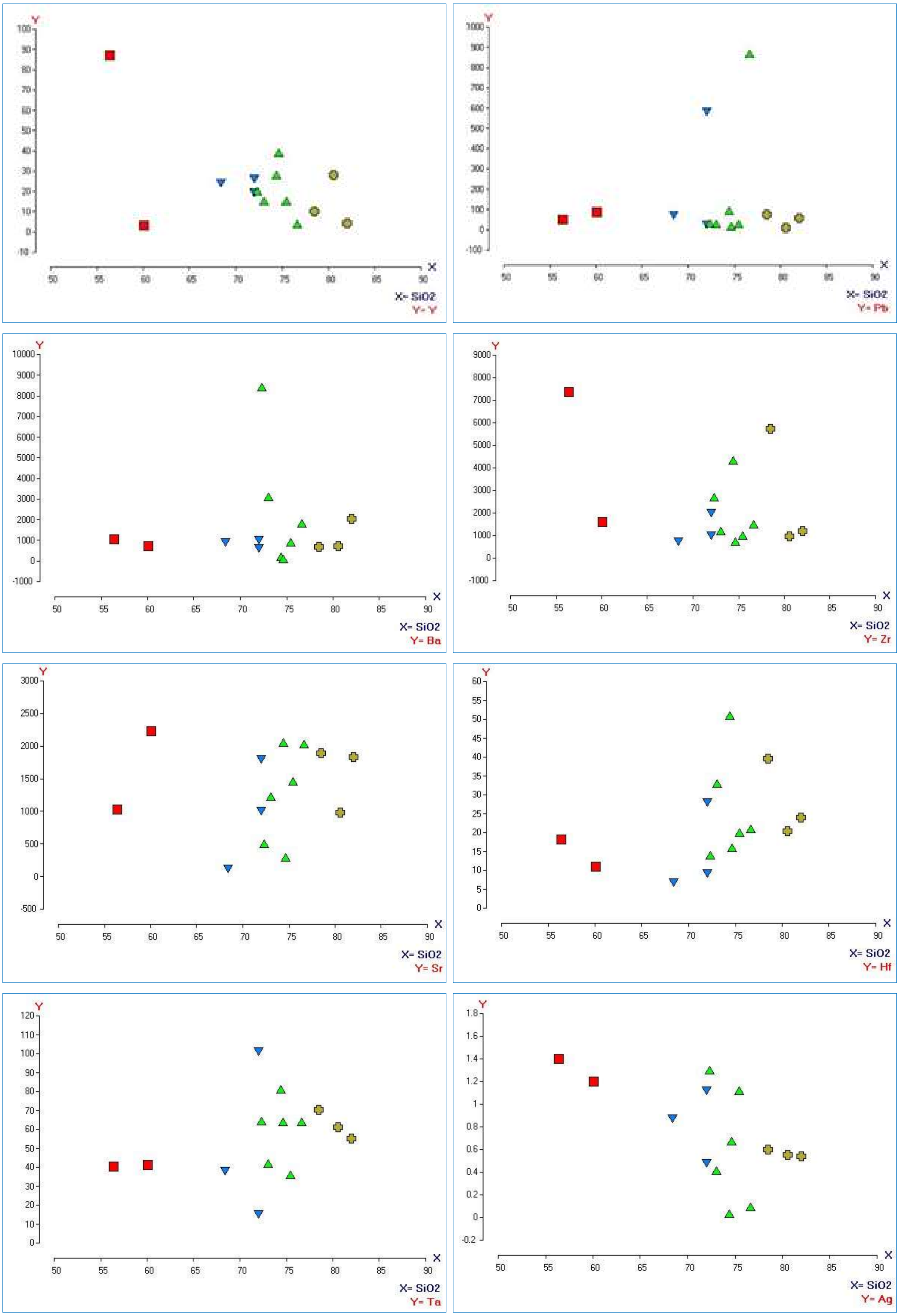
X= SiO2
Y= Y
X= SiO2
Y= Pb
X= SiO2
Y= Ba
X= SiO2
Y= Zr
X= SiO2
Y= Sr
X= SiO2
Y= Hf
X= SiO2
Y= Ta
X= SiO2
Y= Ag

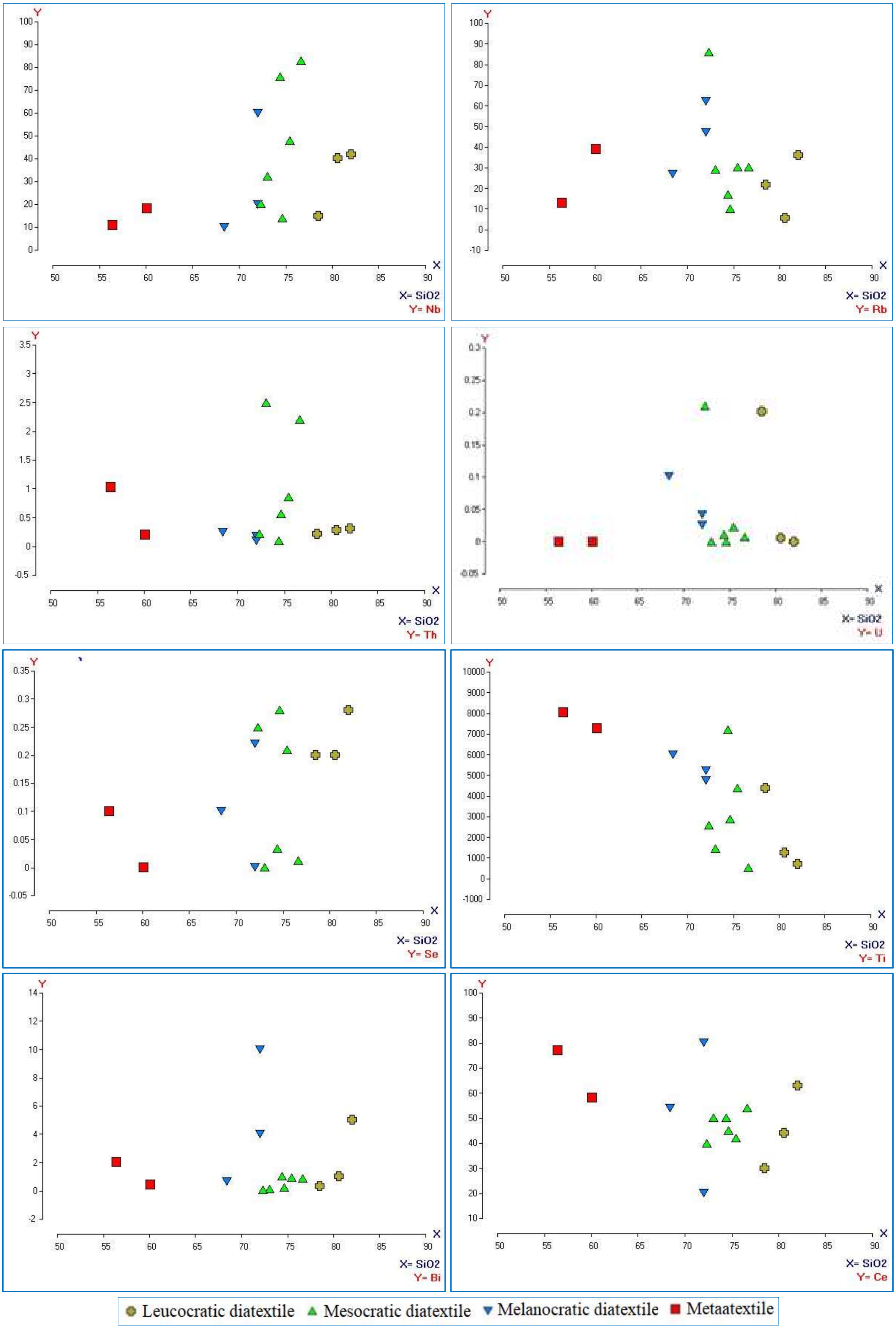

Fig. 9. Plots of trace element contents versus silica for samples from different migmatite site

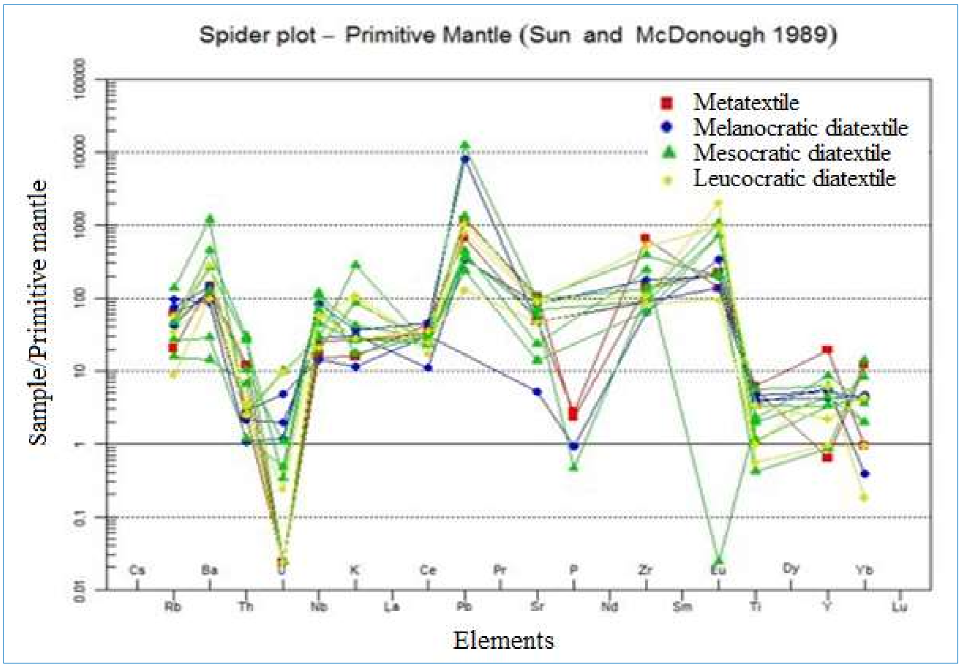

Fig. 10. Multi-element variation diagrams normalized to the primitive mantle values of Taylor and McLennan (1985)

4.2.1. Harker variation diagrams of major oxides and trace elements

In Harker variation diagrams of major oxides (Fig. 7), for most of the samples: MgO, Fe_2O_3, Al_2O_3, CaO, P_2O_5 and TiO_2 decrease with increasing SiO_2, whereas Na_2O and K_2O increase with increasing SiO_2 contents even though some erratic and scattered distributions are also available. This is because MgO, CaO, TiO_2, Fe_2O_3 and Al_2O_3 take part in ferromagnesian minerals formation in initial steps of crystallization, therefore, their concentration decreases with increasing in SiO_2 contents. SiO_2 has positive correlation with Na_2O indicating plagioclase fractionation. SiO_2 shows a good positive correlation with K_2O for most of the samples, supporting the role of fractional crystallization.

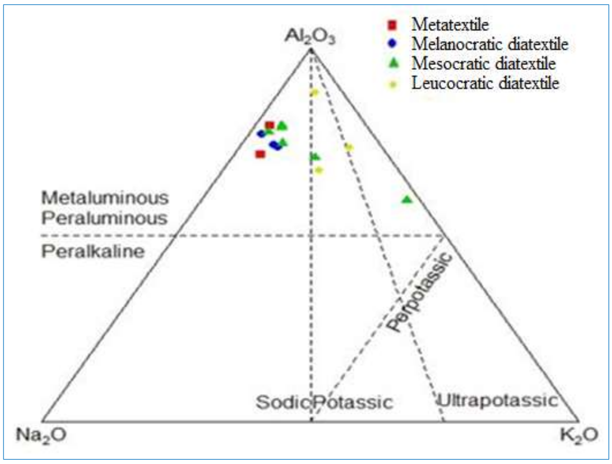

Fig. 11. Molar Na_2O-Al_2O_3-K_2O plot, discriminating metaluminous, peraluminous and peralkaline compositions. Same symbols as used in other geochemical maps

As shown on the Fig. 8, Harker binary plot of A/CNK to SiO_2 has distinctive positive correlation, where A/CNK value increases with the increase of silica values even though some uneven distribution is apparent. Increasing A/CNK with increasing SiO_2 may indicate assimilation of metasedimentary source rock or assimilation and fractional crystallization of a genetically related igneous source with substantial involvement of sedimentary country rock.

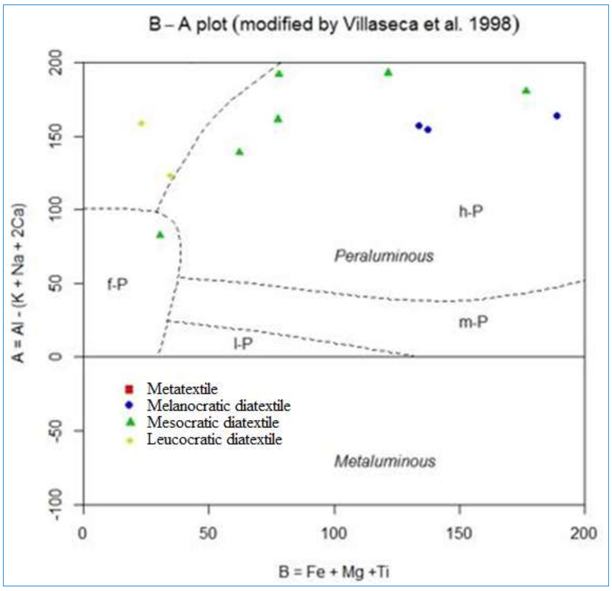

Fig. 12. B-A plot, discriminating metaluminous and peraluminous compositions (modified by Villaseca et al., 1998). Same symbols as used in other geochemical maps

The variation of trace element content examined in relation to the SiO_2 content, as shown in Fig. 9. An obvious feature in the plot is the negative correlations of Ni, Zn, Y, Nb, and Zr with SiO_2, with may indicate that these elements behaved as compatible elements in magmatic fractionation.

Considerable scatter is noted for some other elements, such as Th, Cu, Ba, and Pb. Observing the behavior of these elements, we conclude that Rb, Th, Ba, K, and Pb behaved as incompatible elements; while Ni, Zn, Nb, Zr and Y behaved as compatible elements.

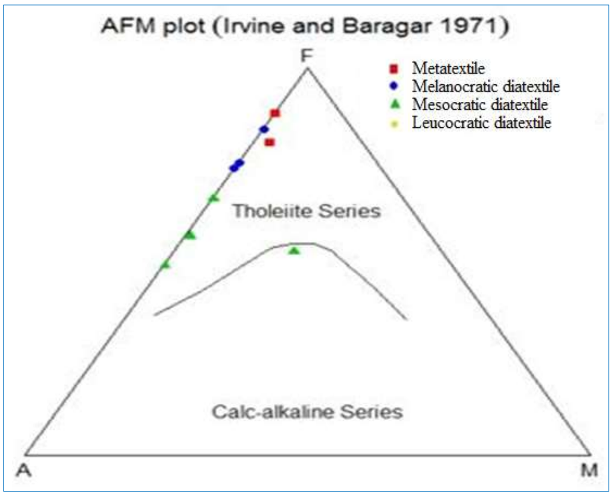

Fig. 13. AFM diagram of Irvine and Baragar (1971) for the analysed migmatite rock samples

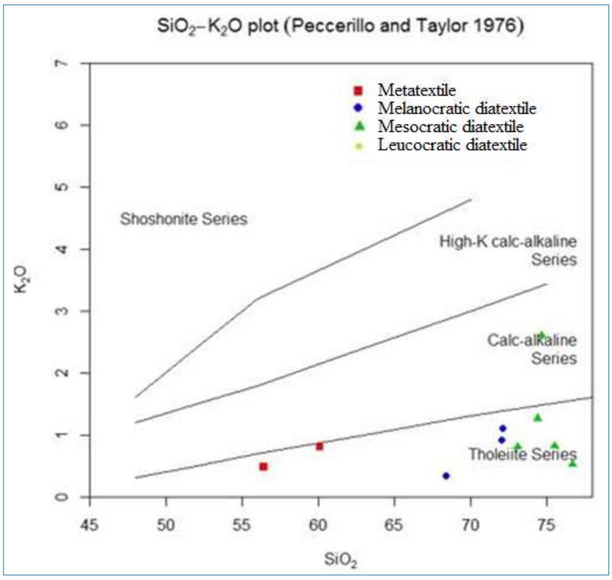

Fig. 14. K_2O vs SiO_2 diagram (after Peccerillo and Taylor, 1976) illustrating the high-theolitic series and calc-alkaline affinities of the analysed migmatite samples. Same symbols as used in other geochemical maps

The B-A plot (Fig. 12) shows that Buzaye migmatites plot within the strong-peraluminous field and one sample fell within felsic peraluminous field. Therefore, the analysed Migmatites samples were defined as completely peraluminous. Based on the plot of AFM classification (Fig. 13) and K_2O vs SiO_2 diagram (Fig. 14) except sample D3 taken from the mesocratic diatexite suite which is magnesium rich falling within calc-alkaline series, all the other samples taken from the migmatite bodies are found within the theoleitic series approaching more to 'F" field because they have relatively higher Fe_2O_3 concentrations.

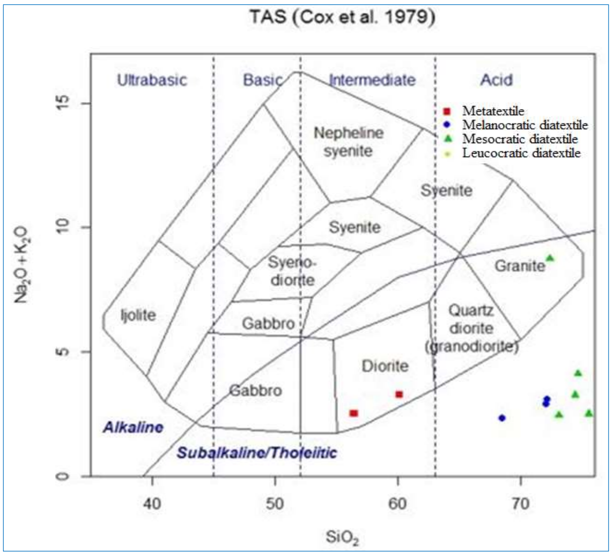

Fig. 15. Geochemical classification diagram (Cox et al., 1979) for migmatite samples. The curved solid line (after Irvine and Baragar, 1971) subdivides the alkalic from subalkalic rocks

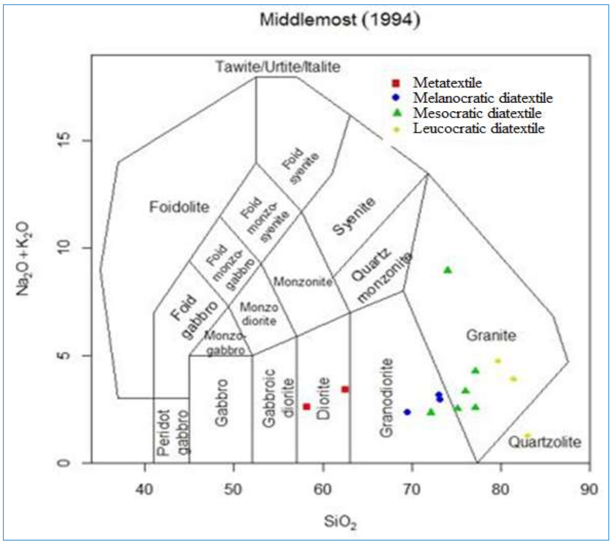

Fig. 16. TAS (Middlemost 1994) classifications of migmatites. Same symbols as used in other geochemical maps

The plotting of the samples in the tholeiitic fields shows that the magma from which the rock was formed was totally restricted in occurrence only to subduction-related environment. This suggests that the migmatites may have been derived mostly from subduction tectonic environment. From the Multi-element variation diagrams (Fig. 10), the overall shape of the individual patterns of all rock types is similar. Broad ranges in compatible elements for the diatexite migmatites are interpreted as being due to K-feldspar dominated fractional crystallization. Therefore, all samples from the study areas show marked negative anomalies in Ti, Yb, P and U and positive anomaly for Nb, Rb, Ba, Th and Pb. Spider diagrams show similar characteristics to those of metatexite and diatexite with negative, P and Ti anomalies, indicating either the retention of plagioclase and accessory minerals in the source during partial melting or their separation during fractionation (Fig. 10).

4.2.2. Geochemical classification of migamatites

Geochemical classification of the analyzed migmatite samples was performed by using: Aluminium saturated index plots, AFM, SiO_2 - K_2O plot of (Peccerillo and Taylor, 1976), TAS (Cox et al., 1979), and TAS (Middlemost, 1994) classification systems.

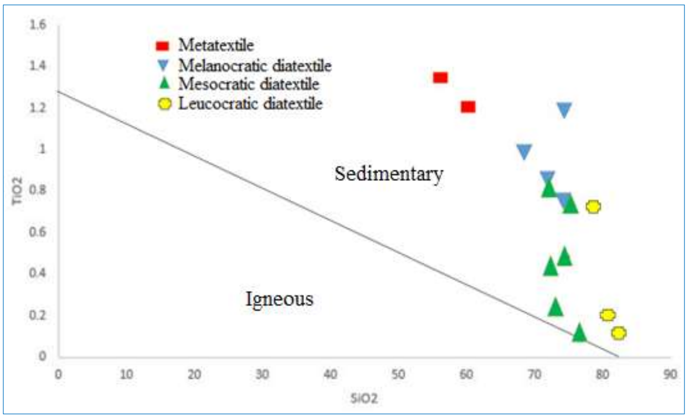

Fig. 17. Discrimination plots of TiO_2 versus SiO_2 after Tarney, 1977. Same symbols as used in other geochemical maps

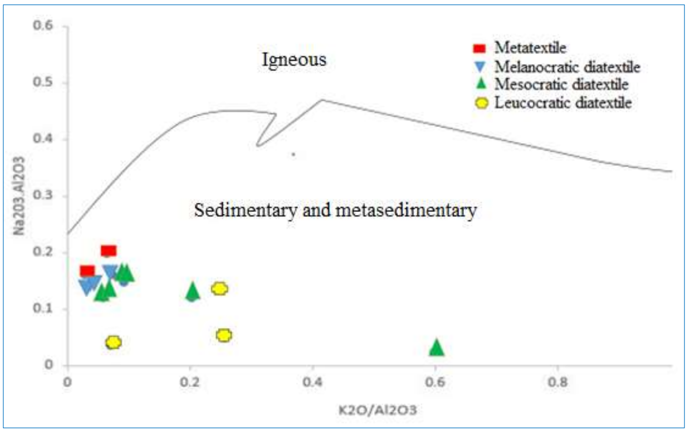

Fig. 18. Na_2O/Al_2O_3 versus K_2O/Al_2O_3 diagram (after Garrels and Mackenzie, 1971). Same symbols as used in other geochemical maps

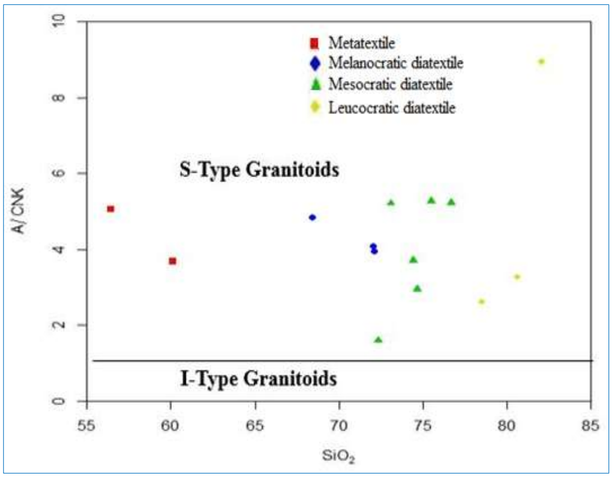

Fig. 19. Molecular $Al_2O_3/Cao+Na_2O+K_2O$ versus SiO_2 diagram showing the classification of the rocks into the fields of I-type and S-type granitoids

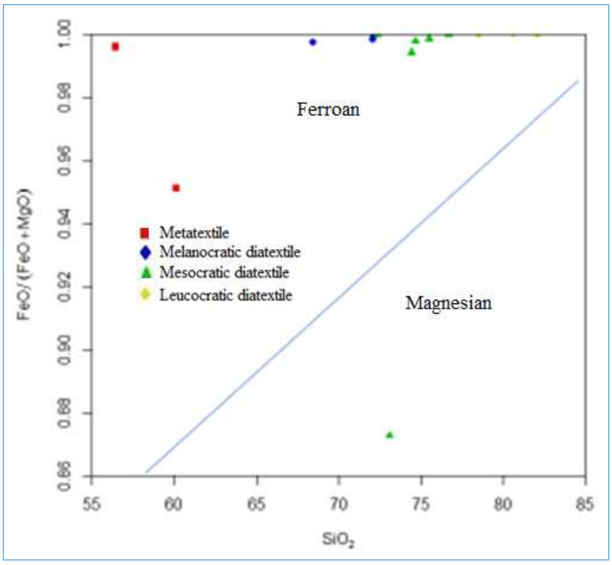

Fig. 20. Plot of tectonic discrimination (Frost et al., 2001). Same symbols with other geochemical plots

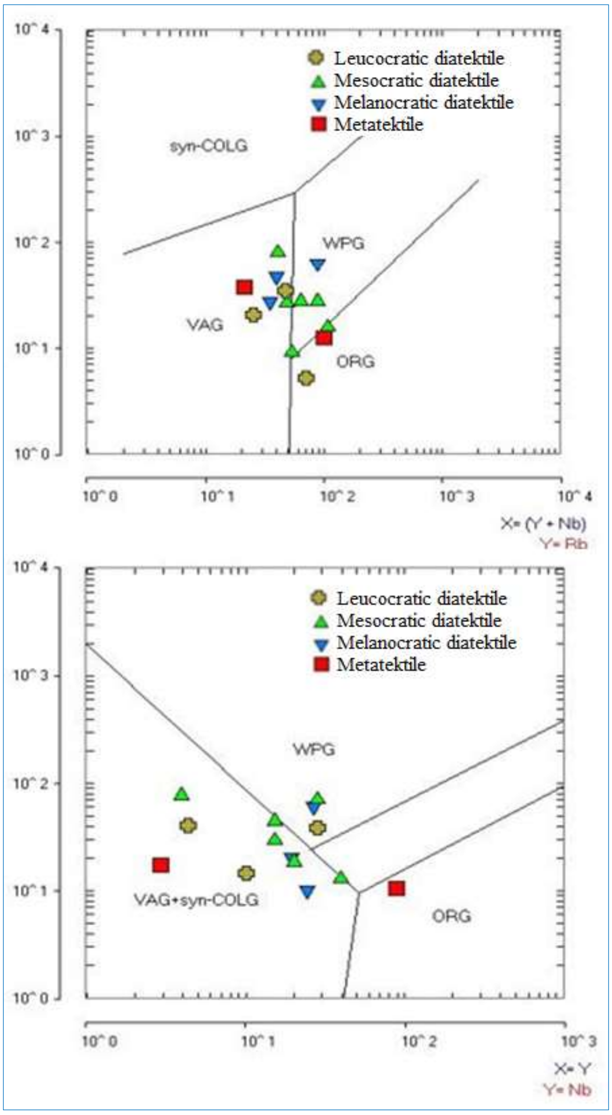

Fig. 21. Plots of Buzaye migmatites on the tectonic discrimination diagram, (a) Rb vs (Y+Nb) of Pearce et al. (1984) and (b) the tectonic discrimination diagram Nb vs Y of Pearce et al. (1984)

From Molar Na_2O-Al_2O_3-K_2O plot (Fig. 11), all the samples were grouped under peraluminous field. Geochemical classification by TAS (Middlemost, 1994) and (Cox et al., 1979) from the migmatites shows that samples from metetexite migmatites were plotted at diorite field and samples from melanocratic diatexites and one sample from mesocratic diatexite falls at the granodiorite field, and samples from leucocratic diatexite falls within granite (Figs. 15-16).

4.3. Source discrimination diagram

A discrimination diagram of TiO_2 versus SiO_2 as proposed by Tarney (1977) and a plot of Na_2O/Al_2O_3 versus K_2O/Al_2O_3 (after Garrels and Mackenzie, 1971) (Figs. 17-18), show that the samples plotted within the sedimentary field an implication that substantial materials may have been generated from sedimentary sources only. Also, the migmatites in the study area fall with S-type garnitoids suggesting that they all have originated from the same metasedimentary protolith (Fig. 19).

4.4. Tectonic settings

Tectonic discrimination classification using major elements (after Frost et al., 2001) shows that all the migmatites samples indicate ferroan, except one sample from mesocratic diatexite (D3) which fall under magnesian due it high magnesium content (Fig. 20).

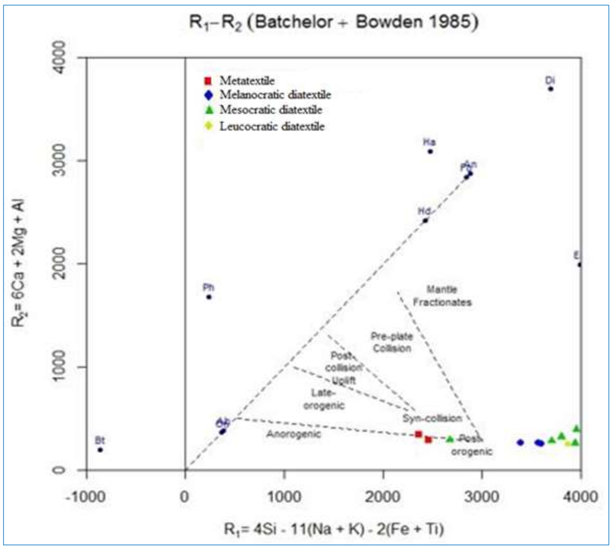

Fig. 22. Multicationic classification plots of De La Roche et al. (1980). (R1: 4Si-11(Na+K)-2(Fe+Ti); R2: 6Ca+2Mg+Al) (Batchelor and Bowden, 1985)

From Fig. 21, the analyzed samples were largely plotted at volcanic arc (VAG) field although some samples plot along the margins of within plate (WPG) field. Some of the samples show transtional character between volcanic arc and within plate granite fields. Based on geotectonic discrimination of Batchelor and Bowden (1985), the analysed samples are plotted in the post orogenic fields with respect to the pan African orogeny (Fig. 22). This generally imply that the migmatites must have been derived from enriched mantle sources and crustal materials involvement and that the migmatites got emplaced during an overlapping tectonic setting related to final stage of orogeny and are said to be late collisional to post collisional migmatites.

5. Conclusion

The study area is part of the granulite facies terrain of the Northern Basement Complex. Field relationship as observed has revealed that the rocks in the study area occur as metatexite and diatexite migmatites based on the morphological classification of Sawyer (2008). Important conclusion obtained in the present study of the Buzaye migmatites may be summarized as follows:

The morphological continuity observed in the field across the paleosome to diatexite transition is mirrored by progressive changes in texture, mineralogy and geochemistry which suggests that anatexis and crustal reworking in the study area occurred as an essentially closed system process.

The negative correlations between Al_2O_3, CaO, P_2O_5, MgO, FeO, MnO, TiO_2 and SiO_2 and positive correlation with Na_2O, K_2O suggest that the leucocratic diatexite rocks are likely the result of fractional crystallization during magmatic evolution, which indicate continuous plagioclase fractionation during metamorphic differentiation.

Based on different geochemical classification systems, all migmatites from the study areas are chemically peraluminous and sub-alkaline (theolitic) in character. The major-trace element geochemistry of the migmatites also suggests that they are S-type, formed in a (volcanic arc) subduction related environments.

Based on tectonic discrimination diagram, the migmatites are ferroan and were plotted at volcanic arc granite and are post orogenic with respect to the Pan-African orogeny.

Melting occurred principally through the dehydration melting of muscovite, and affected virtually the whole succession, as there is very little paleosome preserved; diatexite migmatites is pervasive.

Acknowledgement

This work has evolved out of the Master's thesis of the first author at Abubakar Tafawa Balewa University, Bauchi. The authors are also grateful to all students who assisted during the fieldwork and the anonymous reviewers whose suggestions improved the quality of the paper.

Statements and Declarations

The authors declare that no funds, grants, or other support were received during the preparation of this manuscript. The authors have no relevant financial or non-financial interests to disclose. All authors contributed to the study conception and design. The draft of the manuscript was written by Tahir Garba Ahmad and all authors commented on the manuscript. All authors have read and approved.

References

Attoh, K., 1998. High-pressure granulite facies metamorphism in the Pan-African Dahomeide orogen, West Africa. Journal of Geology 106, 236-246.

Batchelor, R.A., Bowden, P., 1985. Petrogenetic interpretation of granitoid rock series using multi cationic parameters. Chemical Geology 48, 43-55.

Black, R., Liegeois, J.P., 1993. Cratons, mobile belts, alkaline rocks and continental lithospheric mantle: The Pan-African testimony. Journal of the Geological Society 150, 89-98.

Black, R., Latouche, L., Liegeois, J.P., Caby, R., Bertrand, J.M., 1994. Pan-African displaced terranes in the Tuareg shield (central Sahara). Geology 22, 641-644.

Brown, M., 1973. The definition of metatexites, diatexites and migmatites. Proceedings of the Geologists' Association 84, 371-82.

Caby, R., 1989. Precambrian terranes of Benin–Nigeria and Northeast Brazil and the Late Proterozoic South Atlantic fit. Geological Society of America Special Paper 230, 145-158.

Caby, R., 1994. Precambrian coesite from northern Mali: first record and implications for plate tectonics in the trans Saharan segment of the Pan-African belt. European Journal of Mineralogy 6, 235-244.

Caby, R., 2003. Terrane assembly and geodynamic evolution of Central–Western Hoggar: a synthesis. Journal of African Earth Sciences 37, 133-159.

Castaing, C., Triboulet, C., Feybesse, J.L., Chèvremont, P., 1993. Tectonometamorphic evolution of Ghana, Togo and Benin in the light of the Pan-African/Brasiliano orogeny. Tectonophysics 218, 323-342.

Cox, K.G., Bell, J.D., Pankhurst, R.J., 1979. The interpretation of igneous rocks; George Allen and Unwin, London, 450p.

Dada, S.S., Respaut, J.P., 1989. La monzonite à fayalite de Bauchi (bauchite), nouveau témoin d'un magmatisme syntectonique panafricain au nord du Nigéria. Comptes Rendus de l'Académie des Sciences de Paris 309, 887-892.

Dada, S.S., Lancelot, J.R., Briqueu, L., 1989. Age and origin of the annular charnockitic complex at Toro, Northern Nigeria: U–Pb and Rb–Sr evidence. Journal of African Earth Sciences 9, 227-234.

Dada, S., Birck, J.L., Lancelot, J.R., Rahaman, M.A., 1993. Archean migmatite–gneiss complex of North Central Nigeria: its geochemistry, petrogenesis and crustal evolution. International Colloquium on African Geology, Mbabane, Swaziland, 97-102.

Dada, S.S., 1998. Crust-forming ages and proterozoic crustal evolution in Nigeria: a reappraisal of current interpretations. Precambrian Research 87, 65-74.

Djouadi, M.T., Gleizes, G., Ferré, E., Bouchez, J.L., Caby, R., Lesquer, A., 1997. Oblique magmatic structures of two epizonal plutons, Hoggar, Algeria: late-orogenic emplacement in a transcurrent orogen. Tectonophysics 279, 351-374.

Ferre, E.C., Caby, R., Peucat, J.J, Capdevila, R., Monie, P., 1998. Pan-African, post-collisional, ferro-potassic granite and quartz–monzonite plutons of Eastern Nigeria. Lithos 45, 255-279.

Ferre, E.C., Gleizes, G., Caby, R., 2002. Tectonics and post-collisional granite emplacement in an obliquely convergent orogen: The Trans-Saharan belt, Eastern Nigeria. Precambrian Research 114, 199-219.

Ferre, C.E., Caby, R., 2006. Granulite Facies Metamorphism and Charnockite plutonism: Examples from the Neoproterozoic Belt of Northern Nigeria. Journal of Geology 100/06006.

Frost, B.R., Calving, G.B., William, J.C., Richard, J.A., David, J.E., Carrol, D.F. 2001. A geochemical classification for granitic rocks. Journal of Petrology 42 (11), 2033-48.

Garrels, R.M., Mackenzie, F., 1971. Evolution of sedimentary Rock, Norton and Co: New York 394 pp.

Irvine, T.N., Baragar, W.R.A., 1971. A guide to the chemical classification of the common volcanic rocks. Canadian Journal of Earth Sciences8, 523-548.

Jahn, B., Caby, R., Monié, P., 2001. Precambrian UHP eclogites from northern Mali, West Africa: age of UHP metamorphism, nature of protoliths and tectonic implications. Chemical Geology (Isotope Geoscience Section) 178, 143-158.

Liégeois, J.P., Black, R., Navez, J., Latouche, L., 1994. Early and late Pan-African orogenies in the Aïr assembly of terranes (Tuareg shield, Niger). Precambrian Research 67, 59-88.

Middlemost, E.A.K., 1994. Naming materials in the magma/igneous rock system. Earth-Science Reviews 37, 215-224.

Pearce, J.A., Harris, N.B.W., Tindle, A.G., 1984.Trace element Discrimination Diagrams for the Tectonic Interpretation of Granitic Rocks. Journal of Petrology 25 (4), 956-983.

Peccerillo, A., Taylor S.R., 1976.Geochemistry of Eocene calc-alkaline volcanic rocks from the Kastamonu area, Northern Turkey. Contrib Mineral Petrol 58: 63-81.

Sawyer, E.W., 2008. Working with Migmatites. Mineralogical Association of Canada Short Course Series, 38.

Shearer, C.K.., Papike, J.J., Laul, J.C., 1985. Chemistry of Potassium Feldspars from Three Zoned Pegmatites, Black, Hills, South Dakota: Implication Concerning Pegmatite Evolution. Geochemica et Cosmochimica Acta 49, 663-673.

Tarney, J., 1977. Petrology, mineralogy and geochemistry of the Falkland Plateau basement rocks, Site 30, deep sea drilling project. Initial Report, Vol. 36, 893-920.

Taylor, S.R., McLennan, S.M., 1985. The Continental Crust: its composition and evolution. Oxford: Blackwell.

Villaseca, C., Barbero, L., Herreros, V., 1998. A re-examination of the typology of peraluminous granite types in intra continental orogenic belts. Transactions of the Royal Society of Edinburgh, Earth Sciences 89, 113-119.

Wright, E.P., 1971. Basement Complex. In (Geological Survey of Nigeria; ed.). The geology of the Jos Plateau. Geological Survey of Nigeria, Place, 12-47.